

Modeling the Reactivity of Superoxide Reducing Metalloenzymes with a Nitrogen and Sulfur Coordinated Iron Complex

Jason Shearer, Jennifer Nehring, Scott Lovell, Werner Kaminsky, and Julie A. Kovacs*

Department of Chemistry, University of Washington, Seattle, Washington 98195

Received February 26, 2001

Superoxide is a potent cellular poison.¹ As such, organisms have evolved a number of pathways to degrade superoxide before it can cause cellular damage. The best understood are the superoxide dismutases (SOD), which catalyze the disproportionation of superoxide.² In some anaerobic organisms a different protection scheme has evolved. These organisms utilize superoxide reductases (SORs), which catalyze the reduction of superoxide to peroxide, thus eliminating the production of dioxygen.³ Two different SORs have recently been structurally characterized; neelaredoxin (from the hyperthermophilic archeon, *Pyrococcus furiosus*) and rubredoxin oxidoreductase (Rbo, also known as desulfoferredoxin, from *Desulfovibrio desulfuricans*).^{3,4} The active sites of both of these enzymes contain a cysteine-ligated iron center that cycles between the +2 (active form) and +3 (resting form) oxidation states. These lie near the surface of the protein exposed to solvent. In both enzymes, the metal center is five-coordinate in the reduced form and is ligated by four equatorial histidines and one axial cysteine (Scheme 1). Upon oxidation by a protonated superoxide anion, a nearby glutamate residue binds to the metal center in the site *trans* to the cysteine (Scheme 1). Presented below is a five-coordinate Fe(II) complex which models the reactive properties of SORs.

X-ray quality crystals of $[\text{Fe}^{\text{II}}\text{S}^{\text{Me}_2}\text{N}_4(\text{tren})](\text{PF}_6)$ (**1**) were grown from acetonitrile/diethyl ether (1:10) at $-30\text{ }^\circ\text{C}$.^{5,6} The iron center of **1** is in a distorted trigonal bipyramidal environment with the sulfur *trans* to an amine nitrogen in the apical position (Figure 1). All of the bond lengths are typical for an Fe(II) complex in this ligand environment and compare well with those found in the reduced iron center of Rbo.^{4a,f} Complex **1** is five-coordinate, suggesting that small molecules such as HO_2 could possibly bind to, and potentially oxidize the metal center.

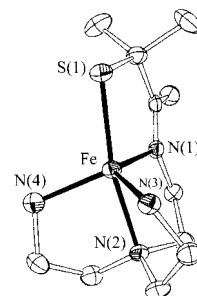
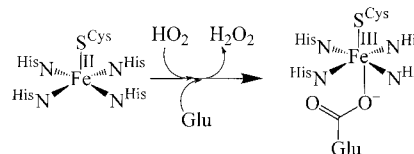


Figure 1. ORTEP of $[\text{Fe}^{\text{II}}\text{S}^{\text{Me}_2}\text{N}_4(\text{tren})]^+$ (**1**) showing 50% probability ellipsoids and atom-labeling scheme. All H atoms have been omitted for clarity. Selected bond lengths for **1**: Fe–N(1), 2.091(3) Å; Fe–N(2), 2.268(3) Å; Fe–N(3), 2.131(3) Å; Fe–N(4), 2.117(3) Å; Fe–S, 2.329(1) Å.

Scheme 1



Upon exposure to a wet acetonitrile solution of potassium superoxide and sodium hexafluorophosphate, the pale yellow-green solution of **1** changes to deep blue (Figure 2).⁷ Furthermore, the resulting solution's electronic absorption spectrum is reminiscent of the oxidized high-pH form of SOR with a λ_{max} at 582 nm ($\epsilon = 1975\text{ M}^{-1}\text{ cm}^{-1}$), suggesting that the solution contained the oxidized form of **1**, possibly with a sixth ligand in the open site.⁴ When this reaction is performed at low temperatures, an intermediate is observed. We are currently in the process of characterizing this intermediate by EXAFS and resonance Raman. This method of generating oxidized **1** was not suitable on a preparative scale, because complete decomposition of the product occurs after a few minutes. This occurs presumably as a result of degradative ligand oxidation by hydrogen peroxide produced in the reaction.⁸

The oxidized form of **1** was rationally synthesized starting from an Fe(III) source. Addition of FeCl_3 in methanol to a methanolic solution of 3-methyl-3-mercaptoputanone and tris(2-aminoethyl)-amine instantly produces a deep blue solution. Exchange of chloride for tetraphenyl borate followed by crystallization from $\text{MeCN}/\text{Et}_2\text{O}$ afforded blue needles. These crystals produced a dark blue solution with an electronic absorption spectrum identical to that of the solution containing **1** and superoxide, and a spectrum similar to that of neelaredoxin and Rbo. The IR spectrum of the

* Author to whom correspondence should be addressed. E-mail: kovacs@chem.washington.edu.

- (1) (a) Totter, J. R. *Proc. Natl. Acad. Sci. U.S.A.* **1980**, *77*, 1763–1767. (b) Burdon, R. H. *Free Radical Biol. Med.* **1995**, *18*, 775–794.
- (2) (a) Lyons, T. J.; Gralla, E. B.; Valentine, J. S. *Met. Ions Biol. Syst.* **1999**, *36*, 125–177. (b) Riley, D. P. *Chem. Rev.* **1999**, *99*, 2573–2587. (c) Culotta, V. C. *Curr. Top. Cell Regul.* **2000**, *36*, 117–132.
- (3) Jenney, F. E., Jr.; Verhagen, M. F.; Cui, X.; Adams, M. W. W. *Science* **1999**, *286*, 306–309.
- (4) (a) Coulter, E. D.; Emerson, J. P.; Kurtz, D. M. Jr.; Cabelli, D. E. *J. Am. Chem. Soc.* **2000**, *122*, 11555–11556. (b) Lombard, M.; Fontecave, M.; Touati, D.; Niviere, V. J. *J. Biol. Chem.* **2000**, *275*, 115–121. (c) Liochev, S. I.; Fridovich, I. *J. Biol. Chem.* **1997**, *272*, 25573–25577. (d) Yeh, A. P.; Hu, Y.; Jenney, F. E., Jr.; Adams, M. W.; Rees, D. C. *Biochemistry* **2000**, *39*, 2499–2508. (e) Chem, L.; Sharma, P.; Le Gall, J.; Mariano, A. M.; Teixeira, M.; Xavier, A. V. *Eur. J. Biochem.* **1994**, *39*, 2499–2508. (f) Coehlo, A. V.; Matias, P.; Fülöp, U.; Thompson, A.; Gonzalez, A.; Carrondo, M. A. *J. Bioinorg. Chem.* **1997**, *2*, 680–689.
- (5) Compound **1** was prepared by combining 2 equiv of 3-methyl-3-mercaptoputanone with ferrous chloride in methanol, adding 1 equiv of tris(2-aminoethyl)amine (tren) followed by stirring for 24 h.
- (6) Crystal data for **1** ($\text{FeC}_{11}\text{H}_{25}\text{N}_4\text{SPF}_6$): brown plates, $0.28 \times 0.16 \times 0.16$ mm, orthorhombic, space group $P2_12_12$, $a = 8.209(2)$ Å, $b = 12.742(1)$ Å, $c = 18.090(2)$ Å, $\alpha = \beta = \gamma = 90^\circ$, $V = 1892(1)$ Å³, $Z = 4$, Mo radiation $\lambda = 0.7107$ Å. For 5636 unique reflections collected at 161 K, the current discrepancy indices are $R = 0.046$ and $R_w = 0.097$ (direct methods using SIR92 software).

- (7) Complex **1** readily reacts with dioxygen to afford a μ -oxo dimer which has been characterized by X-ray crystallography: Shearer, J.; Kaminsky, W.; Kovacs, J. A. Unpublished results.
- (8) The reaction of **1** with superoxide in wet DMSO shows high catalase activity, suggesting that hydrogen peroxide is produced during the reaction. Such high activity is not observed in the absence of **1** and in the presence of **2**. Addition of H_2O_2 to solutions of **2** results in its rapid and complete decomposition.

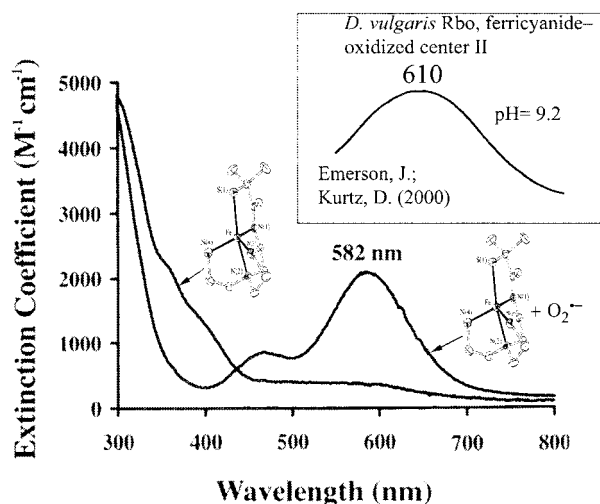


Figure 2. Electronic absorption spectrum of $[\text{Fe}^{\text{III}}\text{SMe}_2\text{N}_4(\text{tren})](\text{PF}_6)$ in MeCN before and after superoxide addition. The spectrum after superoxide addition is identical to that of $[\text{Fe}^{\text{III}}\text{SMe}_2\text{N}_5(\text{TREN})(\text{MeCN})](\text{BPh}_4)_2$ in the 300–1100 nm region. Inset shows the electronic absorption spectrum of Rbo at pH 9.2 (provided courtesy of Emerson and Kurtz).

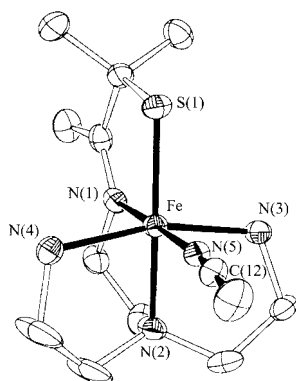


Figure 3. ORTEP of $[\text{Fe}^{\text{III}}\text{SMe}_2\text{N}_5(\text{tren})(\text{MeCN})]^{2+}$ (**2**) showing 50% probability ellipsoids and atom-labeling scheme. All H atoms have been omitted for clarity. Selected bond lengths for **2**: Fe–N(1), 1.911(2) Å; Fe–N(2), 2.026(2) Å; Fe–N(3), 2.001(2) Å; Fe–N(4), 2.018(2) Å; Fe–N(5), 1.948(2) Å; Fe–S, 2.146(1) Å.

solid isolated from this reaction contains a nitrile stretch at 2243 cm^{-1} (vs 2253 cm^{-1} for free MeCN) indicating that the complex is most likely six-coordinate with a bound MeCN ligand. To unambiguously confirm this, X-ray quality crystals were grown from acetonitrile/diethyl ether.

The X-ray crystal structure of $[\text{Fe}^{\text{III}}\text{SMe}_2\text{N}_5(\text{tren})(\text{MeCN})](\text{Ph}_4\text{B})_2\cdot\text{MeCN}$ (**2**) shows that the iron center is contained in a distorted octahedral environment, with one acetonitrile bound *trans* to the imine nitrogen (N(1), see Figure 3).⁹ The Fe–NCMe distance in **2** is 1.95 Å, indicating that there is significant bonding interaction between the Fe and MeCN. The bond lengths in **2** are short for thiolate-ligated Fe(III) complexes, suggesting that it is low-spin ($S = 1/2$). Solid-state magnetic susceptibility measurements indicate **2** has a room temperature $\mu_{\text{eff}} = 2.00 \mu_{\text{B}}$, which is consistent with a low-spin state. In contrast, both neelaredoxin and Rbo contain Fe(III) in a high-spin state ($S = 5/2$),⁴ which is what one would expect for weak-field biological ligands. In solution the bound MeCN of **2** rapidly exchanges with bulk MeCN

as shown by NMR kinetics ($k_{\text{ex}} = 1.21(2) \times 10^{11} \text{ s}^{-1}$ at 20 °C).¹⁰ Preliminary results indicate that the MeCN ligand is easily exchanged by coordinating solvents, such as methanol and pyridine, and anionic ligands, such as azide and cyanide. We are currently investigating the effects of the sixth ligand on the spectroscopic and structural properties of derivatives of **2**. The EPR spectrum of **2**, recorded at 120 K in an acetonitrile/toluene glass, appears axial with g -values typical for low-spin Fe(III) ($g_{\perp} = 2.12$ and $g_{\parallel} = 1.98$). A cyclic voltammogram of **2** recorded in acetonitrile shows a reduction wave that is quasi-reversible with $E_{1/2} = -223 \text{ mV}$ vs SCE, indicating that the Fe(II) state can be accessed through reasonably mild reducing agents.

The possibility that these complexes will act as an SOD was also investigated. Complex **2** shows no immediate reaction with KO_2 in wet MeCN. Instead, the gradual decomposition of **2** is seen after several minutes, affording complete decomposition after about 1 h at room temperature. Also this solution (**2** + KO_2) shows no catalase activity above that of the control reaction (superoxide in wet DMSO). If the oxidized Fe(III) complex was acting as an SOD, thereby generating a reduced Fe(II) complex, this would readily react with protonated superoxide to afford hydrogen peroxide. If O_2 were forming in an SOD reaction, one then would expect to see $[[\text{Fe}^{\text{III}}\text{SMe}_2\text{N}_4(\text{tren})]_2(\mu_2\text{-O})]^{2+}$, a μ -oxo dimer shown to readily form upon exposure of complex **1** to trace amounts of dioxygen.⁷ The fact that no μ -oxo dimer is detected provides further evidence that neither dioxygen nor the Fe(II) product **1** is being produced in the reaction **2** + KO_2 . Therefore, it seems likely that no superoxide oxidation chemistry is taking place. This is despite the fact that superoxide could potentially bind to the metal center of **2** since it has an exchangeable MeCN ligand.

In SORs, SOD activity is probably avoided due to lack of a nearby basic residue to effectively deprotonate superoxide. Basic residues found in the cavities of SODs facilitate the disproportionation reaction. In contrast, SOR active sites rest at the bottom of a shallow cavity near the protein surface, making a proton source readily available, ensuring that superoxide will be protonated throughout catalysis. Also, these models show that SOR activity can occur despite the fact that there is no apparent binding site *trans* to the thiolate sulfur (as is found in the Rbo and neelaredoxin). All iron-containing synthetic systems reported to react with superoxide lack thiolate sulfurs, and most display SOD activity.¹¹ Only a small number of these systems have been reported to display SOR activity.^{11a} The fact that our thiolate-ligated system displays SOR activity suggests that the S^{Cys} of SORs plays an important role in promoting SOR activity. However, the placement of this S^{Cys} relative to the open site (*trans* (enzyme) vs *cis* (model compound **1**)) does not appear to be critical.

Acknowledgment. We wish to thank Dr. Donald M. Kurtz Jr. for thoughtful discussions and access to some unpublished results. Financial support from the NIH (Grant GM 45881) is gratefully appreciated.

Supporting Information Available: Experimental details, crystallographic data for **1** and **2**, and magnetic data (Figure S-1), an EPR spectrum (Figure S-2), a cyclic voltammogram (Figure S-3), and a ^1H NMR spectrum (Figure S-4) for **2**. This material is available free of charge via the Internet at <http://pubs.acs.org>.

IC010221L

(9) Crystal data for **2** ($\text{FeC}_{63}\text{H}_{69}\text{N}_6\text{S}_2$): dichroic (brown-green) prisms, $0.5 \times 0.30 \times 0.27 \text{ mm}$, monoclinic, space group $P2_1/c$, $a = 17.418(2) \text{ \AA}$, $b = 17.749(2) \text{ \AA}$, $c = 17.993(1) \text{ \AA}$, $\alpha = \beta = 90^\circ$, $\gamma = 104^\circ$, $V = 5397(2) \text{ \AA}^3$, $Z = 4$, Mo radiation $\lambda = 0.7107 \text{ \AA}$. For 9032 unique reflections collected at 130 K, the current discrepancy indices are $R = 0.038$ and $R_w = 0.095$ (direct methods using SIR92 software).

(10) Shearer, J.; Jackson, H. L.; Rittenberg, D. K.; Schweitzer, D.; Leary, T. M.; Kaminsky, W.; Scarrow, R. C.; Kovacs, J. A. Manuscript in preparation.

(11) (a) Bernhard, P.; Anson, F. C. *Inorg. Chem.* **1988**, *27*, 4574–4577. (b) Szulbink, W. S.; Warburton, P. R.; Busch, D. H. *Inorg. Chem.* **1993**, *32*, 5368–5376. (c) Bull, C.; McClune, G. J.; Fee, J. A. *J. Am. Chem. Soc.* **1983**, *105*, 5290–5300.